

Dispersion-Relation Calculation of the πN Elastic Scattering Amplitude A' for $-t \leq 0.20 \text{ (GeV/c)}^2$ and $0.575 \leq p \leq 20.0 \text{ GeV/c}^*$

J. A. McClure

Department of Physics, Georgetown University, Washington, D. C. 20007

and

L. E. Pitts

Department of Physics, Mary Washington College, Fredericksburg, Virginia

(Received 16 August 1971)

The method, applicable for small-angle scattering, is based on dispersion relations written for the logarithm of the scattering amplitude and yields an expression for the phase in terms of integrals containing the modulus of the amplitude. Numerical values of the modulus, obtained from unpolarized differential cross-section data, are used as input to the integrals. Techniques are developed for minimizing the effect of the unphysical region and for treating the zeros of the amplitude. Although the primary objective is to calculate the high-energy amplitudes, the method can be used at all lab momenta $p \geq 0.575 \text{ GeV/c}$, and as a check the phases are calculated for $0.575 \leq p \leq 2.07 \text{ GeV/c}$. When the t dependence of the zero of the amplitude is taken into account, the phases, known from partial-wave analyses, are reproduced with discrepancies for π^+p (π^-p) no greater than 3% (9%). The amplitudes A'_l calculated at 2-GeV/c intervals from 2 to 12 GeV/c and at 15, 18, 20, and 30 GeV/c at squared momentum transfers of $-t = 0.0, 0.025, 0.05, 0.10, 0.15, 0.20 \text{ (GeV/c)}^2$ are presented.

I. INTRODUCTION

Fixed-momentum-transfer pion-nucleon dispersion relations are based on the Hilbert transforms

$$\text{Re}F(\nu, t) = \frac{1}{\pi} P \int \frac{\text{Im}F(\nu', t) d\nu'}{\nu' - \nu}, \quad (1a)$$

$$\text{Im}F(\nu, t) = -\frac{1}{\pi} P \int \frac{\text{Re}F(\nu', t) d\nu'}{\nu' - \nu}, \quad (1b)$$

which are an immediate consequence of the analyticity of the function $F(\nu, t)$ in the energy variable $\nu = (s - u)/M$. Here s , u , and t are the usual Mandelstam variables¹ and M is the nucleon mass. Dispersion relations have proven most useful in those cases where either the real or imaginary part of the amplitude can be obtained from experiment and the most important instance is $F = f(\nu, 0)$ with f the laboratory spin-nonflip amplitude. The analyticity of the function rests on generally acceptable assumptions, such as unitarity, crossing symmetry, and microcausality, and its imaginary part is directly related to the experimentally measured total cross section by the optical theorem.² The successful comparison of the theoretical results with the forward πN scattering amplitude measured by Lindenbaum and co-workers³ is one of the major accomplishments of the analytic S-matrix approach and is of fundamental significance as verification of some of the basic axioms

of elementary-particle physics.

For nonforward scattering $t \neq 0$ the usefulness of the Eqs. (1) is drastically reduced because the optical theorem no longer applies and neither $\text{Im}f$ nor $\text{Re}f$ can be measured experimentally. Therefore, it has been suggested^{4, 5} that instead of writing the dispersion relation of the amplitude $F = |f|e^{i\phi}$, it should be written for the logarithm

$$F = \ln f = \ln |f| + i\phi. \quad (2)$$

Assuming the required behavior at infinity (as given in Sec. II), Eq. (1b) becomes

$$\phi(\nu, t) = -\frac{1}{\pi} P \int \frac{\ln |f(\nu', t)| d\nu'}{\nu' - \nu}, \quad (3)$$

which will be referred to as a logarithmic dispersion relation LDR. This form has the advantage that in some instances it is possible to measure $|f(\nu, t)|$ directly. This is the case for πN elastic scattering where the unpolarized cross section is

$$\frac{d\sigma}{d\Omega} = |f(\nu, t)|^2 + |g(\nu, t)|^2$$

with g the spin-flip amplitude. Near the forward direction, the cross section involves only the spin-nonflip amplitude

$$\frac{d\sigma}{d\Omega} \approx |f(\nu, t)|^2, \quad (4)$$

an approximation which tends to be valid to larger values of t as energy increases. At high energies

the t dependence of $|f|$ is of the form⁶

$$|f(\nu, t)| \approx |f(\nu, 0)| e^{a(\nu)t + b(\nu)t^2}, \quad (5)$$

with $a(\nu)$ and $b(\nu)$ experimentally known functions of energy. Equation (5) follows from the well-known diffraction peak observed in the differential cross section. At lower energies $|f|$ can be constructed from existing partial-wave analyses. Thus, over the great part of the physical region, for small t , $|f|$ is experimentally available as input for the integral (3).

Since $|f|$ must be known for this approach to work and the amplitude in the usual form can be obtained from

$$\text{Re}f = |f| \cos \phi,$$

$$\text{Im}f = |f| \sin \phi,$$

emphasis will, therefore, be placed on the calculation of the phase ϕ .

We have undertaken a program aimed at making the LDR a useful theoretical tool for the calculation of scattering amplitudes near the forward direction, and this paper reports the first results of that effort. There are two major difficulties encountered in using this technique. The first is the presence of an unphysical region where no information about the amplitude's modulus can be obtained from experiment. This difficulty is also encountered in conventional dispersion relations.⁷ The other, unique to this problem, is that the zeros of the amplitude are singularities of its logarithm and, therefore, a knowledge of the location of these zeros is required for the evaluation of Eq. (3). We have developed techniques for surmounting these difficulties, and they will be discussed in detail in the following sections.

The objective is to calculate the small-angle πN phase for energies above the region where partial-wave analyses are feasible. As far as we know, this cannot presently be accomplished in a model-independent way. Philosophically, the ideal in this calculation has been the well-known forward dispersion relations which, aside from the asymptotic behavior of the total cross section, seem to rest on a minimum of generally acceptable assumptions. For this effort, a relatively small angular interval has been taken $-t \leq 0.2 (\text{GeV}/c)^2$. In a subsequent calculation, an extension of the results out to $0.6 (\text{GeV}/c)^2$ will be attempted.

II. SUBTRACTED LDR

It is convenient to use the invariant amplitudes A' and B rather than f and g because of their properties under crossing symmetry,⁸

$$|A'_\pm(\nu, t)| = |A'_\pm(-\nu, t)|.$$

Throughout subsequent sections, the notation \pm shall refer to $\pi^\pm p$. The unpolarized cross section, in terms of these variables, is

$$\frac{d\sigma}{d\Omega} = \left(\frac{M}{4\pi W}\right)^2 \left[\left(1 - \frac{t}{4M^2}\right) |A'|^2 + \frac{t}{4M^2} \left(s - \frac{(\nu+M-t/4M)^2}{1-t/4M^2}\right) |B|^2 \right], \quad (6)$$

where $A'(\nu, 0) = 4\pi f(\nu, 0)$ and $W = s^{1/2}$.

The amplitude $A'(\nu, t)$ at fixed t , regarded as a function of the complex energy ν , is analytic in the upper plane, has cuts along the real axis from thresholds at $\pm\nu_1$ ($\nu_1 = \mu + t/4M$) to $\pm\infty$, and has the usual nucleon poles at $\lambda_\pm = \mp(\mu^2/2M + t/4M)$ on the axis between thresholds. Here μ is the mass of the pion. A' can be expressed in terms of other amplitudes, A and B ,

$$A' = A + \left(\frac{\nu}{1-t/4M^2}\right) B,$$

which have been shown to have the asymptotic behavior² at fixed t

$$\nu^{-1} |A(\nu, t)| < K, \quad |B(\nu, t)| < K' \quad \text{as } \nu \rightarrow \infty,$$

whence

$$\nu^{-1} |A'(\nu, t)| < K'' \quad \text{as } \nu \rightarrow \infty, \quad (7)$$

where K , K' , and K'' are constants. Let us assume that at small t the phase of $A'(\nu, t)$ is bounded for large ν and that $A'(\nu, t)$ does not fall off more rapidly than some power of ν^{-1} . Both of these assumptions are valid at $t=0$. Then Eq. (7) implies

$$\frac{\ln A'(\nu, t)}{(\nu^2 - \nu_1^2)^{1/2}} \rightarrow 0 \quad \text{as } \nu \rightarrow \infty$$

which with Eq. (8) insures the vanishing of the contribution of the infinite contour as is required in the derivation of Eqs. (1).

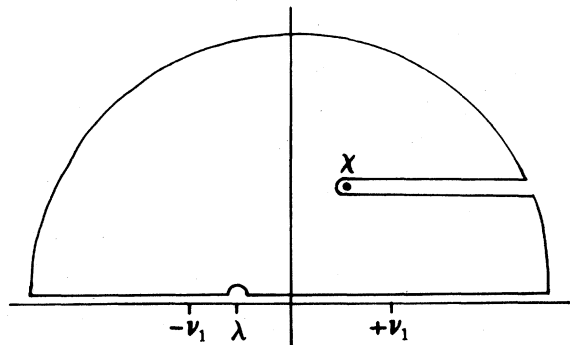


FIG. 1. Contour in the complex energy plane used in the derivation of Eq. (9).

A' may, in general, have zeros anywhere in the complex energy plane, but for reasons to be presented in Sec. IV, we shall assume it has no real zeros and only one, located at χ , in the upper half plane. Under these conditions, application of Eq. (1b) to the function

$$F(\nu, t) = \frac{\ln A'(\nu, t)}{(\nu^2 - \nu_1^2)^{1/2}} \quad (8)$$

at fixed t on the contour shown in Fig. 1 yields the more complete version of Eq. (3) which we write for ϕ_- , a similar expression holding for ϕ_+ :

$$\begin{aligned} \phi_-(\nu, t) = & -\frac{(\nu^2 - \nu_1^2)^{1/2}}{\pi} \left(P \int_{\nu_1}^{\infty} \frac{\ln |A'_+(\nu', t)| d\nu'}{(\nu' + \nu)(\nu'^2 - \nu_1^2)^{1/2}} + P \int_{\nu_1}^{\infty} \frac{\ln |A'_-(\nu', t)| d\nu'}{(\nu' - \nu)(\nu'^2 - \nu_1^2)^{1/2}} \right) + [\phi_-(\nu_1, t) - \phi_+(\nu_1, t)] \\ & - \sin^{-1} \left(\frac{\nu_1^2 - \nu\lambda_-}{\nu_1(\lambda_- - \nu)} \right) - 2 \operatorname{Im} \ln \left(\frac{-\nu_1^2 + \nu\chi + (\nu^2 - \nu_1^2)^{1/2}(\chi^2 - \nu_1^2)^{1/2}}{(\nu^2 - \nu_1^2)^{1/2}(\chi - \nu)} \right). \end{aligned} \quad (9)$$

For details of the derivation see Ref. 4. The factor $(\nu^2 - \nu_1^2)^{-1/2}$ serves two important purposes; it makes the integrand imaginary between thresholds and it ensures convergence of the integrals at the upper limit.

Initial calculations were made with Eq. (9), but it was found that it gave poor results for $t \neq 0$ (as determined by our checking procedure in Sec. V). The difficulty was a large contribution to the integrals from the unphysical region $\nu_1 < \nu' < \mu$. The values of A' obtained by the Lehmann continuation are very large, probably too large, and the contribution is magnified by the factor $(\nu^2 - \nu_1^2)^{-1/2}$ which is large for ν' small.

We have attacked this problem by trying to arrange the calculation in such a way that the unphysical region does not give much of a contribution no matter what values of A' are (within reason). This was accomplished by using a subtraction procedure with

$$F(\nu, t) = \frac{(\nu^2 - \nu_1^2)^{1/2} \ln A'(\nu, t)}{(\nu - \nu_0)(\nu + \nu_0)}. \quad (10)$$

The factor $(\nu^2 - \nu_1^2)^{1/2}$, which is still needed, is retained in the numerator where it will tend to reduce rather than exaggerate the contribution of the poorly known unphysical region, and the high-energy convergence is restored by subtracting the LDR at $\pm\nu_0$. ν_0 is chosen near the upper end of the partial-wave region where the subtraction constants introduced $\phi_{\pm}(\nu_0, t)$ are available from the partial-wave analysis. The net effect of this change is to shift the weighting of the integrals away from the very low energies to the middle and upper partial-wave regions where, presumably, the input data are most accurate. The new form of the LDR is

$$\begin{aligned} \phi_-(\nu, t) = & \left(\frac{\nu_0^2 - \nu_1^2}{\nu^2 - \nu_1^2} \right)^{1/2} \left(\frac{\nu + \nu_0}{2\nu_0} \phi_-(\nu_0, t) - \frac{\nu - \nu_0}{2\nu_0} \phi_+(\nu_0, t) \right) \\ & + \frac{\nu^2 - \nu_0^2}{\pi(\nu^2 - \nu_1^2)^{1/2}} \left(P \int_{\nu_1}^{\infty} \frac{(\nu'^2 - \nu_1^2)^{1/2} \ln |A'_+(\nu', t)| d\nu'}{(\nu' + \nu)(\nu'^2 - \nu_0^2)} - P \int_{\nu_1}^{\infty} \frac{(\nu'^2 - \nu_1^2)^{1/2} \ln |A'_-(\nu', t)| d\nu'}{(\nu' - \nu)(\nu'^2 - \nu_0^2)} \right) \\ & + \frac{1}{2} \left[1 - \frac{\nu}{\nu_0} \left(\frac{\nu_0^2 - \nu_1^2}{\nu^2 - \nu_1^2} \right)^{1/2} \right] [\phi_-(\nu_1, t) - \phi_+(\nu_1, t)] - \sin^{-1} \left(\frac{\nu_1^2 - \nu\lambda_-}{\nu_1(\lambda_- - \nu)} \right) \\ & - \left(\frac{\nu_0^2 - \nu_1^2}{\nu^2 - \nu_1^2} \right)^{1/2} \left[\frac{\nu_0 - \nu}{2\nu_0} \sin^{-1} \left(\frac{\nu_1^2 + \nu_0\lambda_-}{\nu_1(\nu_0 + \lambda_-)} \right) + \frac{\nu_0 + \nu}{2\nu_0} \sin^{-1} \left(\frac{\nu_1^2 - \nu_0\lambda_-}{\nu_1(\nu_0 - \lambda_-)} \right) \right] \\ & - \pi \frac{\nu - \nu_0}{\nu_0} \left(\frac{\nu_0^2 - \nu_1^2}{\nu^2 - \nu_1^2} \right)^{1/2} - 2 \operatorname{Im} \ln \left(\frac{-\nu_1^2 + \nu\chi + (\nu^2 - \nu_1^2)^{1/2}(\chi^2 - \nu_1^2)^{1/2}}{(\nu^2 - \nu_1^2)^{1/2}(\chi - \nu)} \right) \\ & + \left(\frac{\nu_0^2 - \nu_1^2}{\nu^2 - \nu_1^2} \right)^{1/2} \left[\frac{\nu + \nu_0}{\nu_0} \operatorname{Im} \ln \left(\frac{-\nu_1^2 + \nu_0\chi + (\nu_0^2 - \nu_1^2)^{1/2}(\chi^2 - \nu_1^2)^{1/2}}{(\nu_0^2 - \nu_1^2)^{1/2}(\chi - \nu_0)} \right) \right. \\ & \left. + \frac{\nu - \nu_0}{\nu_0} \operatorname{Im} \ln \left(\frac{-\nu_1^2 - \nu_0\chi - (\nu_0^2 - \nu_1^2)^{1/2}(\chi^2 - \nu_1^2)^{1/2}}{(\nu_0^2 - \nu_1^2)^{1/2}(\chi + \nu_0)} \right) \right]. \end{aligned} \quad (11)$$

While this new expression involves more terms than Eq. (9) it is not different in any essential way. It does, however, require as experimental input the values of $\phi_{\pm}(\nu_0, t)$.

III. $A'(\nu, t)$ AS INPUT DATA

The values of A' used in the integrals can be divided into four parts according to the energy range. A' is in units of F .

(i) *Resonance region* $\mu < \nu < 2 \text{ GeV}$. At these energies the amplitudes vary most rapidly and they are obtained by reconstruction from existing partial-wave analyses, particularly that of Wagner.⁹ For pion lab momentum $p < 4.0 \text{ GeV}/c$ this part of the range of integration gives the major contribution of the integrals to the LDR.

(ii) *Diffraction-peak region* $2 < \nu < 24 \text{ GeV}$. Near the forward direction, the differential cross section (6) reduces to its first term and at higher energies this cross section is observed to fall off exponentially with t as

$$\frac{d\sigma}{d\Omega} = \left(\frac{d\sigma}{d\Omega} \right)_{t=0} e^{at+bt^2} \approx \left(\frac{M}{4\pi W} \right)^2 \left(1 - \frac{t}{4M^2} \right) |A'|^2.$$

Therefore,

$$|A'(\nu, t)| = \frac{|A'(\nu, 0)| e^{(at+bt^2)/2}}{(1-t/4M^2)^{1/2}}, \quad (12)$$

where a and b are weakly energy-dependent.⁶ From approximately 2 to 24 GeV (π^-p) and 16 GeV (π^+p), the cross sections¹⁰ were fitted to the form (12) and values of $A'(\nu, 0)$, $a(\nu)$, and $b(\nu)$ were obtained. The $A'(\nu, 0)$ obtained by this process of extrapolating the differential cross section to the forward direction are slightly different from those calculated from the optical theorem via the forward dispersion relations.

(iii) *Very high energies* $\nu > 24 \text{ GeV}$. Above 24 GeV no angular data are available and, as is the case with forward dispersion relations, some assumptions must be made about the behavior of the amplitude in this range. a and b are observed to be nearly constant for $p > 8 \text{ GeV}$, and their average values are used at higher energies.

Forward dispersion relations have shown that above 25 GeV the contribution of the real part to $A'(\nu, 0)$ is less than 2%, and we have, therefore, approximated A' by its imaginary part.³ This was obtained through the optical theorem from Carter's fit to the total cross section,¹¹

$$\sigma = \sigma_\infty + Bp^\alpha \quad (13)$$

with

$$\begin{aligned} \sigma_\infty &= 21.8, & B_+ &= 21.85, & \alpha_+ &= -0.90, \\ B_- &= 23.75, & \alpha_- &= -0.70. \end{aligned}$$

Assumptions about the very-high-energy region, which can readily be changed as new data become available, impose an upper limit on the energy at which the LDR can be used with confidence. We find that above 12 GeV this region makes a con-

siderable contribution to the integrals, and it should be remembered that the phases calculated at 15, 18, 20, and 30 GeV/ c are sensitive to the details of the assumed asymptotic behavior.

(iv) *Unphysical region* $\nu_1 < \nu < \mu$. For $t \neq 0$ there is a short range of energy just above threshold for which $\cos\theta < -1$ and the scattering is not a physically realizable process. This problem is well known in ordinary dispersion relations and the standard method of obtaining the amplitude in this region is through analytic continuation of the partial-wave expansion as proposed by Lehmann.⁷ Our amplitudes are constructed in this way although the values of ν and t are outside the range for which this procedure has been proven to converge. However, the subtraction procedure will be shown to damp any contribution to the integrals to an acceptable value.

IV. LOCATION OF THE ZERO

The complications caused by zeros of the amplitude present one of the major obstacles in any attempt to make practical use of logarithmic dispersion relations. The problem arises because the logarithm is singular at a zero of the amplitude, giving rise to the χ -dependent terms in Eq. (11). To numerically evaluate such a term it is necessary to know the location of the zero in the complex energy plane, a location which depends on t . While a few properties of the zeros can be proven, e.g., that some exist, there is no practical way of locating them for an arbitrary t .

The function $A'(\nu, t)$ for fixed t is completely determined all over the complex plane by the value of its imaginary part along the real axis through the conventional dispersion relations,

$$\begin{aligned} A'_\pm &= - \left(\frac{G_r^2}{M} \right) \frac{1}{\nu - \lambda_\pm} + \int_{\nu_1}^{\infty} \frac{\text{Im}A'_\pm(\nu', t) d\nu'}{\nu - \nu'} \\ &+ \int_{\nu_1}^{\infty} \frac{\text{Im}A'_\mp(\nu', t) d\nu'}{\nu + \nu'}, \end{aligned} \quad (14)$$

where we have written the unsubtracted version for simplicity. Here G_r^2 is the πN coupling constant squared. In the work of Jorna and McClure¹² this equation with values of the imaginary part from the optical theorem was employed to locate the zeros of the forward πN amplitudes. With the fact that $\text{Im}A'_\pm(\nu, 0)$ is positive for all energies and reasonable assumptions about the asymptotic behavior, it was shown with the aid of the phase representation¹³ that there is only one complex zero in the upper plane. This was located (at 0.132 and 0.096 GeV) and it was found that there were no zeros on the real axis between thresholds. As a practical matter, it was observed in the com-

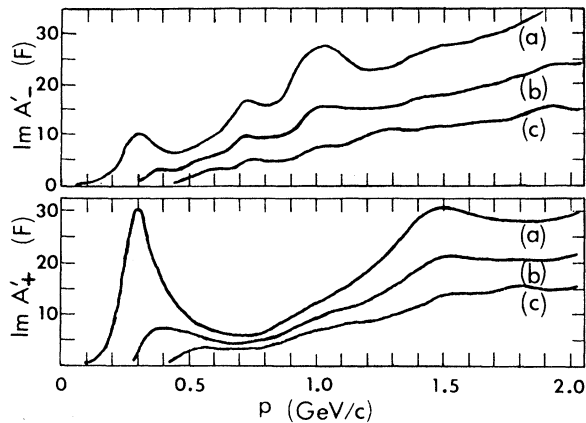


FIG. 2. $\text{Im } A'_l(\nu, t)$ at partial-wave energies for various momentum transfers. Curves (a), (b), and (c) correspond, respectively, to $-t=0, 0.1, \text{ and } 0.2 \text{ (GeV/c)}^2$.

putation of Ref. 10 that a key factor in there being only one zero was the positive definiteness of $\text{Im } A'_l(\nu, 0)$. As ν varies from the zero in a given direction, the real and imaginary parts of the function generated by Eq. (14) tend to move monotonically away from zero. For nonforward angles, lacking a way to obtain $\text{Im } A'_l(\nu, t)$ for all energies, a numerical zero search cannot be carried out.

The location and number of zeros is determined through Eq. (14) by the imaginary part of A' . For

small values of t such as are considered in this investigation, it is reasonable that the zero situation is not very different from that at $t=0$. To support this view, we have calculated $\text{Im } A'_l(\nu, t)$ from the partial waves for several values of t from threshold to $\approx 2.0 \text{ GeV}$. This is shown in Fig. 2. It is clear that while there is significant change in $\text{Im } A'_l(\nu, t)$ as t increases, enough to make the zero of the function generated from it through Eq. (14) shift, the over-all behavior of the function is the same. For example, it remains positive over the great part of the energy range. Because of the generally similar structure of $\text{Im } A'_l(\nu, t)$ for $-t \leq 0.2 \text{ (GeV/c)}^2$ and for reasons to be discussed in Sec. V(ii), we have made the assumption that for small t values there is only a single zero which moves as t changes. The question of zeros will be discussed further in Sec. VI.

V. NUMERICAL EVALUATION AT LOW ENERGIES AND IN THE FORWARD DIRECTION

There are two numerical checks by which the LDR can be tested: the forward direction at any experimentally practical energy and nonforward scattering in the partial-wave region.

(i) *Forward scattering.* At $t=0$ the input data discussed in Sec. III are sufficient for the evaluation of Eq. (11). There is no troublesome unphysical region and the location of the zero is exactly known. The subtraction point was taken

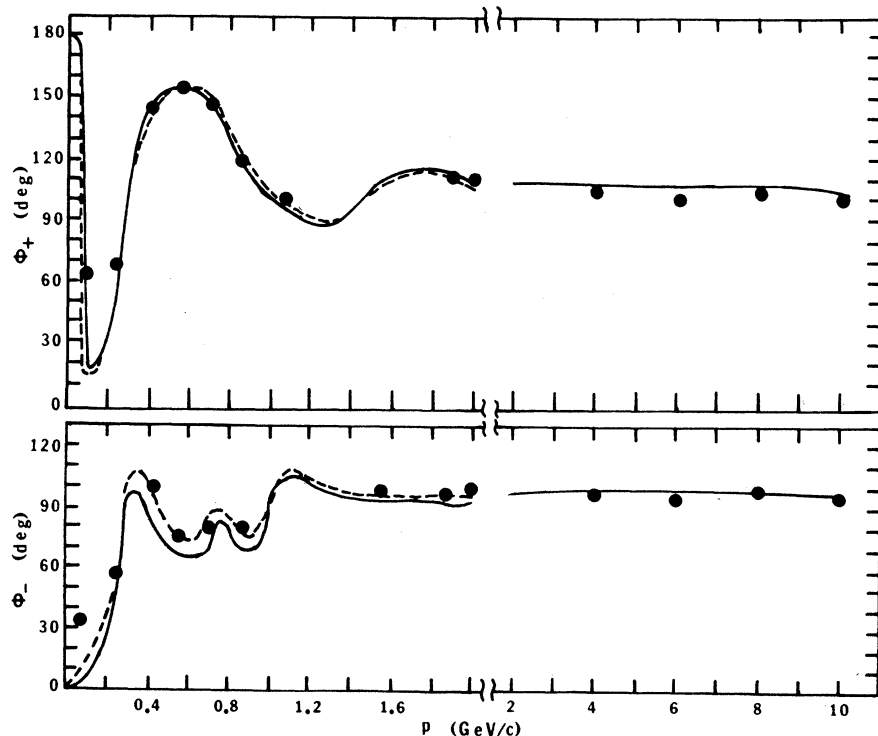


FIG. 3. The forward phases $\phi_{\pm}(\nu, 0)$. The points are calculated with the LDR Eq. (11). The dashed and solid curves are, respectively, the partial-wave and forward-dispersion-relation results.

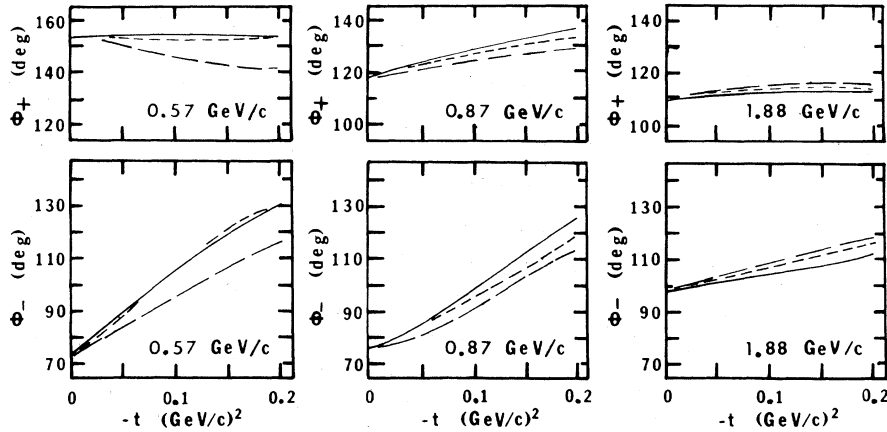


FIG. 4. The phases $\phi_{\pm}(\nu, t)$ at partial-wave energies. The solid curve is obtained from partial-wave analyses. The long-dashed and short-dashed curves are calculated with Eq. (11) using the zeros $\chi(0)$ and $\chi(t)$, respectively. The χ 's are discussed in Sec. V(ii).

at $p=1.278$ GeV/c. For comparison, values of $\text{Re}A'$ and $\text{Im}A'$ are available from partial-wave analyses for $p \leq 2.07$ GeV/c and from conventional forward dispersion relations for higher momenta, both being in substantial agreement with experiment. Our LDR forward phases for both $\pi^{\pm}p$ are shown in Fig. 3 compared with these two. The agreement is quite good except for $p < 0.1$ GeV/c, where ϕ_{-} tends to be too large. The principal-value integrals are quite sensitive to the behavior of the integrand, and at these lowest energies $\ln A'$ varies rapidly. We believe the disagreement here is due to our parametrization of the data and does not reflect any fundamental shortcoming of the method.

There is generally better agreement for $\pi^{+}p$ than $\pi^{-}p$, a result which we also find to hold true in the nonforward-scattering check. This taken in light of the rather substantial disagreement seen in Fig. 3 between the partial-wave and the conventional dispersion-relation phases suggests that the input data for $\pi^{+}p$ may be more reliable than $\pi^{-}p$.

(ii) *Nonforward scattering.* From partial-wave analyses, the amplitudes $A'(\nu, t)$ have been reconstructed, both modulus and phase, from threshold to $p=2.07$ GeV/c and for $0 \leq -t \leq 0.20$ (GeV/c) 2 . While our main objective is to calculate the high-energy phases, the LDR gives them at all energies and, as a further check, we can require that it reproduce these known ones in the partial-wave region. All necessary input data except the location of the zero are provided by the procedures of Sec. III, and as a first approximation we assumed that the zero remained fixed at its $t=0$ location.¹² The results of this calculation are shown in Fig. 4 as the long-dashed curve. It is obvious from the figures that there is a systematic discrepancy between our results and the partial-wave values for both $\pi^{\pm}p$. The phases calculated with the fixed

zero $\chi(0)$ are too small below the subtraction energy and too large above.

The subtraction procedure, introduced in Sec. II to damp the contribution of the unphysical region, has reduced it to a maximum of 5% (π^{+}) of the total phase at $p=0.575$ GeV/c and $-t=0.20$ (GeV/c) 2 and as the energy increases this percentage steadily decreases. Thus, the subtraction procedure is quite successful in reducing the effects of the unphysical region and is, we feel, one of the more important results of our study. Below $p=0.575$ GeV/c the unphysical region becomes increasingly important, agreement with the partial waves is poor, and this momentum roughly defines the limit below which the LDR is not reliable. For phases at partial-wave energies, the contribution from the asymptotic region is largest at $p=2.07$ GeV/c where it reaches a maximum of 15% (π^{-}). Thus, the contributions of the unphysical and asymptotic regions, where assumptions were necessary, are both relatively small in the partial-wave region.

This process of elimination strongly suggests

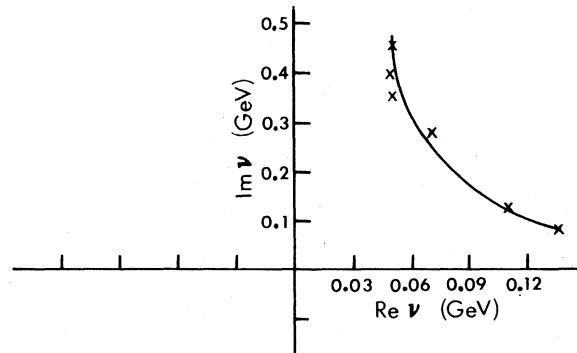


FIG. 5. Locus of the zero $\chi(t)$ of the amplitude $A'_{\nu}(t)$ in the complex energy plane.

TABLE I. The phases $\phi_{\pm}(\nu, t)$ of the amplitudes $A'_{\pm}(\nu, t)$ as given by Eq. (11) using the zeros $\chi(t)$. At each p and t the upper number is ϕ (deg) and the lower $|A'|$ (F).

p (GeV/c)	$-t$ (GeV/c) ²	0.00	0.025	0.05	0.10	0.15	0.20
A'_-							
0.57		73	80	89	105	118	131
		8.9	7.7	6.8	5.3	4.2	3.2
0.71		78	81	85	94	104	116
		16.7	14.6	12.8	9.8	7.5	5.7
0.87		76	80	84	94	105	117
		18.0	15.4	13.2	9.7	7.3	5.6
1.58		100	102	104	108	112	116
		28.3	25.7	23.4	19.3	16.0	13.2
1.88		98	101	103	107	112	116
		34.2	31.3	28.7	24.0	20.0	16.5
2.00		99	102	104	109	114	118
		36.6	33.1	30.0	24.4	19.8	16.0
2.07		101	103	105	109	113	116
		37.8	34.3	31.0	25.2	20.3	16.2
4.0		100	102	104	107	111	113
		61.3	55.4	50.1	41.0	33.7	27.7
6.0		96	98	101	106	110	113
		83.2	75.5	68.5	56.4	46.5	38.3
8.0		98	100	101	105	107	111
		114.7	102.2	91.2	69.7	55.9	47.5
10.0		96	98	100	103	106	109
		143.3	127.7	113.9	91.0	73.1	59.0
12.0		97	99	101	104	106	108
		162.4	145.0	129.6	103.9	83.7	67.8
15.0		103	104	105	107	109	110
		214.0	189.1	167.5	132.0	104.8	83.8
18.0		99	101	102	104	105	106
		225.5	202.0	181.1	146.2	118.6	96.6
20.0		99	101	101	103	106	106
		270.1	240.8	215.1	172.3	138.9	112.7
30.0		98	101	105	106	107	109
		364.8	324.2	288.5	229.7	184.0	148.4
A'_+							
0.57		155	153	155	153	153	154
		15.7	14.9	14.0	12.1	10.0	7.9
0.87		118	120	123	127	130	133
		9.6	9.2	8.9	8.1	7.5	6.8
1.88		112	112	113	113	114	113
		30.1	28.0	25.9	22.2	18.9	16.0
2.00		109	110	110	111	111	111
		30.9	28.6	26.5	22.8	19.4	16.6
2.07		108	109	109	110	111	111
		32.5	30.5	27.9	23.9	20.3	17.3
4.0		107	108	108	109	109	109
		56.6	52.0	47.8	40.3	34.0	28.7
6.0		101	102	102	103	105	106
		87.3	78.5	70.8	57.7	47.3	38.9
8.0		104	104	103	103	104	104
		106.0	95.7	86.5	70.9	58.3	48.2
10.0		103	103	102	103	103	103
		139.0	116.0	111.5	89.9	72.8	58.3
12.0		104	104	103	102	102	103
		146.3	131.5	118.7	96.2	78.7	64.6
15.0		106	105	104	103	103	103
		204.1	182.0	162.4	130.0	104.7	84.7
18.0		106	105	104	103	103	102
		213.6	191.5	171.8	139.0	113.1	92.5
20.0		104	105	102	104	103	104
		235.9	211.4	189.7	153.5	124.9	102.2
30.0		99	100	97	91	91	100
		347.0	311.0	279.1	225.7	183.7	150.3

that the systematic discrepancy seen in Fig. 4 is due to the neglected t dependence of the zero terms. Under this assumption we have found, at each t , values of $\chi = \chi_1 + i\chi_2$ which best remove this difference. This is actually quite a stringent requirement because the two real numbers χ_1 and χ_2 fix the location of the zeros of both A'_+ and A'_- , since these are symmetric with respect to the imaginary axis.¹² Once chosen at a given t , they must remove the discrepancy in both amplitudes for all energies in the partial-wave region. Further, the functional dependence of the phase given in Eq. (11) on the zero location is through rather complicated logarithmic functions, and there is no assurance beforehand that any choice of χ will improve both ϕ_+ and ϕ_- . Finally, the zeros so determined, regarded as functions of t , must move in the complex energy plane in a continuous way from the known $t=0$ location.

The values of (χ_1, χ_2) which best remove the discrepancy were found to be (0.11, 0.13), (0.07, 0.28), (0.05, 0.35), (0.05, 0.40), and (0.05, 0.45) for $-t = 0.025, 0.05, 0.10, 0.15,$ and 0.20 (GeV/c)², respectively. Their locus in the energy plane is shown in Fig. 5. Reevaluation of the LDR (11) with the new zero locations yielded much improved values of the phases, particularly ϕ_+ where the difference from the partial-wave values was reduced to less than 3% at all energies (the new phases are shown in Fig. 4 as the short-dashed line). The improvement was generally less dramatic for ϕ_- where differences ranged up to 9%

at $p=2.07$ GeV/c. Again, as was noted for the forward direction, this may be due to the uncertainties in the π^-p data. With the zeros now fixed for each t value and the other input data as discussed in Sec. III, the phases are completely determined by Eq. (11) for all energies.

VI. HIGH-ENERGY RESULTS AND CONCLUSIONS

Our objective is to obtain the small-angle phases, ϕ_{\pm} , for energies above the partial-wave region, and this calculation can now be accomplished. We have concentrated on the range $2.0 \leq p \leq 12.0$ GeV/c calculating the phases at six t values at intervals of 2.0 GeV/c. The results vary slowly and uniformly with energy, and interpolations within these intervals can be made with reasonable confidence. Phases are also presented for $p=15, 18, 20,$ and 30 GeV/c, but at these higher energies the results are strongly dependent on the assumptions made about the asymptotic region and they should be viewed with appropriate caution. All results are given in Table I, including those in the partial-wave region. Also listed for convenience are $|A'_{\pm}|$, the latter at diffraction energies being obtained between data points by linear interpolation. Because Eq. (11) is quite long, a breakdown of the contributions of the various types of terms at several energies is given in Table II. The angular dependence of both phases and moduli at a sequence of fixed energies is shown in Fig. 6. Part of our motivation in developing the LDR

TABLE II. Contributions to the total phase ϕ_{\pm} of the different types of terms appearing in Eq. (11). The terms are grouped as follows: Those depending on the (A) threshold phase $\phi_{\pm}(\nu_1, t)$, (B) location of the pole λ_{\pm} , (C) location of the zero $\chi(t)$, (D) subtraction-point phase $\phi_{\pm}(\nu_0, t)$, (E) direct integrals over $\ln|A'_{\pm}(\nu, t)|$, (F) crossed integrals over $\ln|A'_{\mp}(\nu, t)|$. All entries are in degrees.

p (GeV/c)	$-t$ (GeV/c) ²	A	B	C	D	E	F	ϕ_-	ϕ_+
0.57	0.0	2.1	-0.4	-227.7	221.0	-20.8	99.1	73	
		-2.1	0.0	-216.6	209.7	76.0	87.6		155
	0.2	1.0	-0.8	-229.3	266.0	15.4	79.1	131	
1.88		-1.0	-0.6	-221.6	262.5	29.7	84.7		154
	0.0	-0.3	0.0	58.3	71.1	7.3	-38.2	98	
		0.3	0.0	56.8	60.1	29.9	-35.2		112
4.00	0.2	-0.1	0.1	59.2	78.1	9.4	-30.8	116	
		0.1	0.1	57.6	74.7	12.4	-31.5		113
	0.0	-0.5	0.1	123.8	36.3	47.2	-107.3	100	
8.00		0.5	0.0	121.2	25.3	61.3	-101.3		107
	0.2	-0.2	0.2	125.3	37.1	38.7	-87.7	113	
		0.2	0.1	122.1	33.7	41.2	-88.3		109
8.00	0.0	-0.5	0.1	152.6	20.9	95.3	-170.6	98	
		0.5	0.0	149.9	9.9	106.8	-163.4		104
	0.2	-0.2	0.2	153.4	19.3	77.2	-139.3	111	
		0.2	0.1	150.4	15.9	77.9	-140.7		104

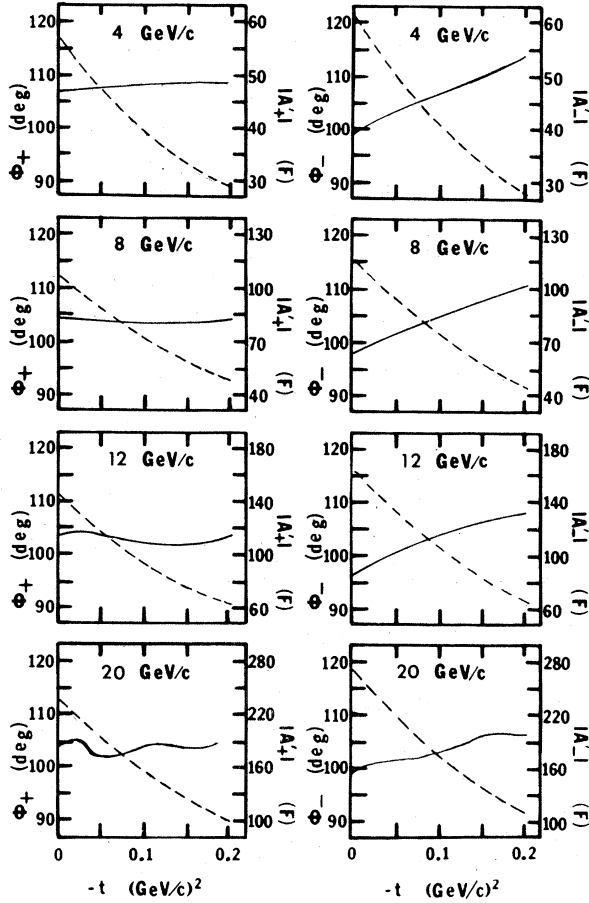


FIG. 6. The high-energy phases $\phi_{\pm}(\nu, t)$ calculated with Eq. (11) (solid curve) and the magnitudes $|A'_i(\nu, t)|$ (dashed curve).

$$\int \frac{(\nu'^2 - \nu_1^2)^{1/2} \ln |A'(\nu', t)| d\nu'}{(\nu' + \nu)(\nu'^2 - \nu_0^2)} \approx \int \frac{(\nu'^2 - \nu_1^2)^{1/2} \ln |A'(\nu', 0)| d\nu'}{(\nu' + \nu)(\nu'^2 - \nu_0^2)} + \int \frac{(\nu'^2 - \nu_1^2)^{1/2} (at + bt^2) d\nu'}{(\nu' + \nu)(\nu'^2 - \nu_0^2)} \quad (15)$$

in which the first term to a good approximation is that associated with the forward direction. Thus

$$\phi(\nu, t) - \phi(\nu, 0) \approx t \int \frac{(\nu'^2 - \nu_1^2)^{1/2} a(\nu') d\nu'}{(\nu' + \nu)(\nu'^2 - \nu_0^2)} + t^2 \int \frac{(\nu'^2 - \nu_1^2)^{1/2} b(\nu') d\nu'}{(\nu' + \nu)(\nu'^2 - \nu_0^2)}. \quad (16)$$

For $-t \leq 0.20$ (GeV/c)² only the first term is significant, but for larger t values the second, of opposite sign, becomes important. On the basis of this term alone, we would expect ϕ_- , say, to rise more slowly and eventually decrease.

Viewed in perspective, what we have attempted to do in this paper is to make a first application of the logarithmic dispersion relation (3) in a practical situation. The successful calculation of the known forward phases, Fig. 3, indicates the basic soundness of the method. The major aim, however, is to exploit the potential of this

method was to find an independent way of checking the widely used Regge-pole theory and these phases invite comparison, but we will not do so here.

The LDR shows that because of analyticity, the phases of A'_i are in the main determined by their moduli, and it is interesting to note that differences between A'_i are more pronounced in the phase than in the modulus. Although $|A'_i|$ is somewhat larger in the forward direction than $|A_i|$ and falls more rapidly with increasing t , the so-called crossover effect, the two are not greatly different. On the other hand ϕ_+ is nearly flat with changing t at 4.0 GeV/c developing a downward slope at higher momenta, while ϕ_- rises from the forward direction with very little change as energy increases. It may also be noted that at 20 GeV/c a dip around $-t = 0.05$ (GeV/c)² begins to appear in ϕ_+ , and to a lesser extent in ϕ_- . It is even more pronounced at 30 GeV/c. This dip appears to be a consequence of our assumption that the exponential behavior (12) persists to much higher energies with approximately the same values of $a(\nu)$ and $b(\nu)$. If this effect is real and not an artifact of faulty asymptotic assumptions, it may be observable in very high energy, small-angle polarization measurements.

If the idea that the phase is determined by the modulus is pursued, a change in t dependence with increasing t can be anticipated from the behavior of the integrals which are the major contributors in Eq. (11). The exponential falloff of A' , Eq. (12), implies for a typical integral, neglecting the slightest t dependence in the denominator,

technique for the determination of nonforward amplitudes. Ways of overcoming the various difficulties encountered have been presented, some more successful than others. The subtraction procedure is quite effective in reducing the influence of the unphysical region at high energy; its contribution is less than 0.5% for $p > 4.0$ GeV/c. The zeros do not seem to be a serious problem for A' over this angular range because it has only one zero in the forward direction and, at the small t values considered here, this situation almost certainly persists. That we can choose a reasonable

locus for this single zero which almost completely removes the discrepancy in ϕ_+ , and to a somewhat lesser extent in ϕ_- , across the partial-wave region is consistent with there being only one. Nevertheless, the behavior of the zeros at nonforward angles is an assumption and is apt to be more troublesome as the calculation is extended to larger t . Presently, we are working on ways of handling this difficulty.

The method is, of course, limited by the available experimental input and, as noted in Sec. V, the comparison of ϕ_- from the partial waves and forward dispersion relations raises some question about the π^-p data. Our results could be affected either through errors in $|A_-|$ or in the subtraction-

point phase $\phi_-(\nu_0, t)$. Another limitation for high-energy applications comes from the asymptotic region. The integrals in the LDR depend strongly on the value of $|A'|$ in the neighborhood of the principal-value point, and the higher the energy the more critical is the assumed behavior of $|A'|$. A modification of the function F as given by Eq. (10), which will lessen the dependence of this region while retaining the virtues of the subtraction, is being sought.

In the immediate future we plan to extend this calculation to $-t = 0.40$ (GeV/c)² and later to make applications of the LDR to Kp scattering and to πN polarization.

*Based in part on a M. S. thesis submitted by L. E. Pitts to Georgetown University.

¹G. F. Chew, *S-Matrix Theory of Strong Interactions* (Benjamin, New York, 1962).

²J. Hamilton and W. S. Woolcock, *Rev. Mod. Phys.* **35**, 737 (1963).

³S. J. Lindenbaum, in *Pion-Nucleon Scattering*, edited by G. L. Shaw and D. Y. Wong (Wiley, New York, 1969), p. 81.

⁴R. Odorico, *Nuovo Cimento* **54**, 96 (1968).

⁵J. A. McClure and S. Jorna, *Nuovo Cimento* **67A**, 667 (1970).

⁶L. Bertocchi and E. Ferrari, in *High Energy Physics*,

edited by E. H. S. Burhop (Academic, New York, 1967), Vol. 2.

⁷H. Lehmann, *Nuovo Cimento* **10**, 579 (1958).

⁸V. Singh, *Phys. Rev.* **129**, 1889 (1963).

⁹D. J. Herndon, A. Barbaro-Galtieri, and A. H. Rosenfeld, Particle Data Group, Lawrence Radiation Laboratory report (unpublished).

¹⁰Geoffrey C. Fox and C. Quigg, LRL Report No. UCRL 20001 (unpublished).

¹¹A. A. Carter, Cavendish Laboratory report, Cambridge, England (unpublished).

¹²S. Jorna and J. A. McClure, *Nucl. Phys.* **B13**, 68 (1969).

¹³M. Sugawara and A. Tubis, *Phys. Rev.* **130**, 2127 (1963).

Nonleptonic Hyperon Decays in a Current-Current Quark Model*

Michael Gronau

California Institute of Technology, Pasadena, California 91109

(Received 6 July 1971)

The symmetric quark model is used to provide an explanation of the S - and P -wave nonleptonic hyperon decays. The current-algebra approach, applied to the current-current weak Hamiltonian constructed of Bose-type quark fields, leads to a remarkable agreement with experiment.

I. INTRODUCTION

The universal current-current theory of the weak interactions¹ has been successful in describing the leptonic and semileptonic weak processes. However, attempts made to apply the theory to the nonleptonic decays led to considerable disagreement with observations.² It appears as if the application of symmetry principles such as $SU(3)$ and CP invariance and the assumptions of current algebra and partial conservation of axial-vector current

(PCAC) cannot always explain the empirical $|\Delta I| = \frac{1}{2}$ rule observed in all these processes. Moreover, even when octet dominance is assumed, direct application of soft-pion techniques to the nonleptonic hyperon decays leaves us with the wrong ratio of P - to S -wave amplitudes.³

It is believed in general that with the above assumptions one can fairly well describe the main features of S -wave amplitudes, while the P waves cannot be understood through similar techniques since they involve some delicate limiting proce-